4.4. Building a conceptual regional geological and geophysical model

4.4.1.2. Building synoptic geophysical images over the study area

4.4.1.2.1. General considerations. Data coverage and filtering

Following the acquisition and processing of geophysical data, the main objective was to obtain the first large-scale synoptic images covering the entire studied area. This was possible through the integration of data gathered during three field campaigns of the project with previous gravity and geomagnetic data available publicly. Figure 4.4.1.2.1 presents the data coverage in the surveyed area.

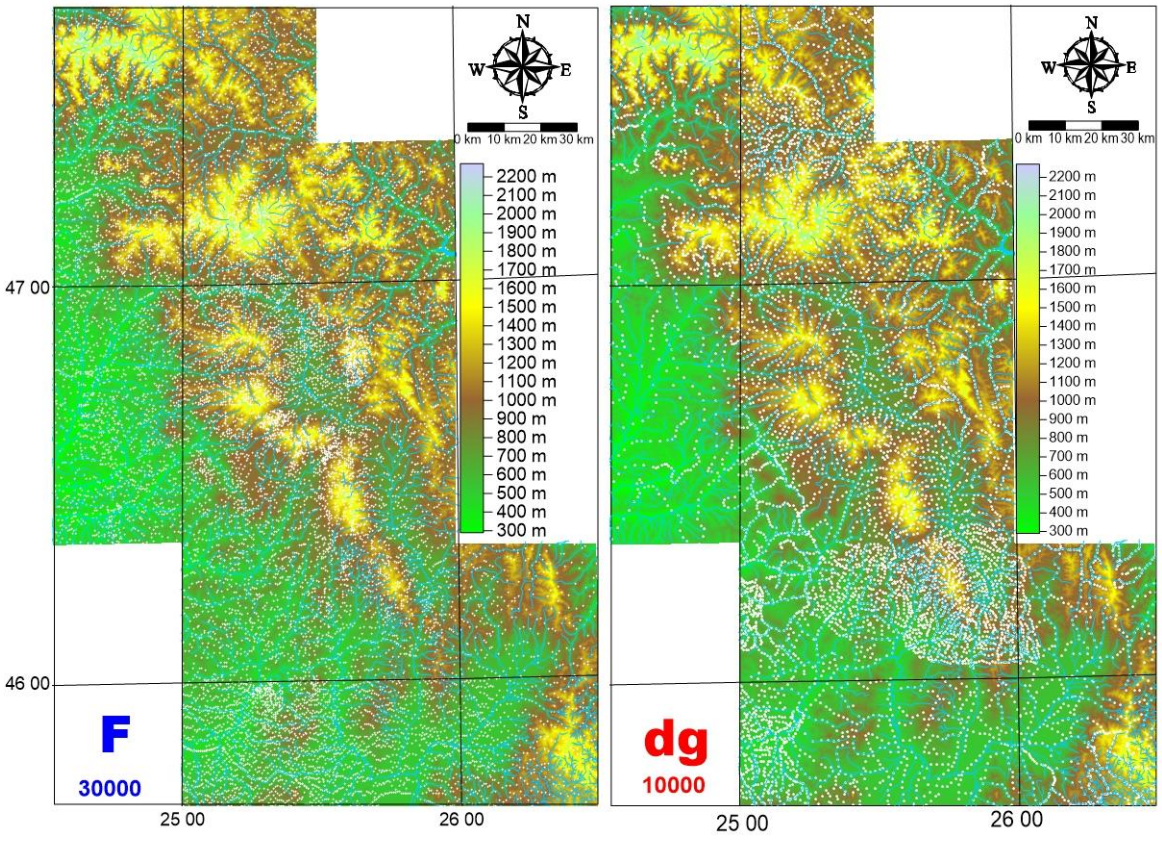

Fig. 4.4.1.2.1 Topography model and the coverage with gravity and geomagnetic observations of the study area. White dots mark the data point locations

The first large scale synoptic geophysical images over the whole area of the Neogene to Quaternary volcanism of East Carpathians (NQECV) are represented by the maps of the geomagnetic anomaly and Bouguer anomaly (Fig. 4.4.1.2.2).

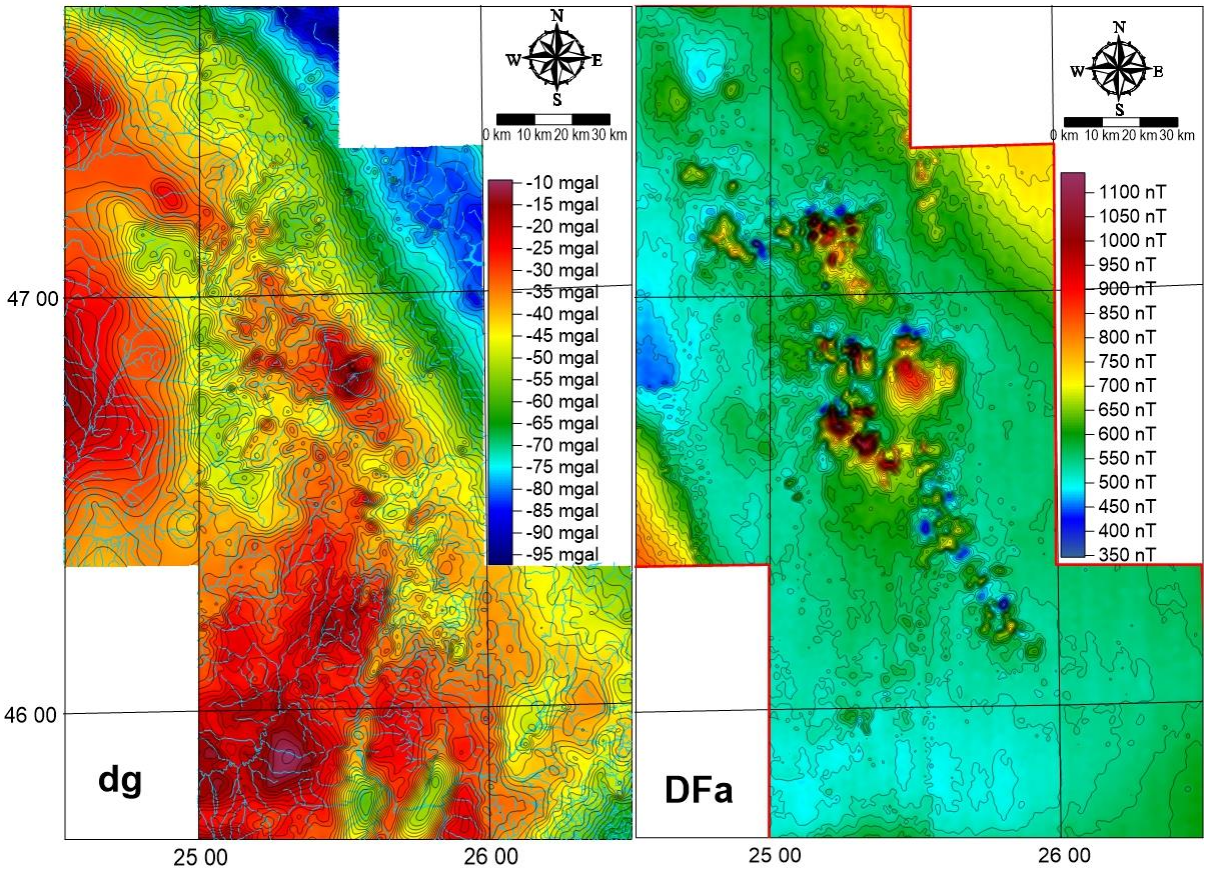

Fig. 4.4.1.2.2 Composite maps of the geomagnetic and Bouguer anomaly over the NQECV area

Unfortunately, the images are strongly unbalanced, being affected among others by effects of some large-scale sources located laterally outside the NQECV area. For instances, the Bouguer anomaly is strongly influenced by the mass contrasts generated by the Transylvanian Basin to the west, and East Carpathians foredeep to the east, while the geomagnetic anomaly is largely distorted by major sources located at various levels in the Transylvanian Basin and the area of the Brodina-Bicaz regional anomaly). Noise produced by shallow local sources, as well as the acquisition and/or processing errors also need to be mitigated.

To provide an appropriate balance to the gravity and geomagnetic effects, the regional effects produced by the above-mentioned laterally located sources have been mitigated through computing and removing from the observations some polynomial trends. The images provided in the figure 4.4.1.2.3 have been obtained after removing a second

order polynomial trend from geomagnetic data and a third order polynomial trend from the gravity data.

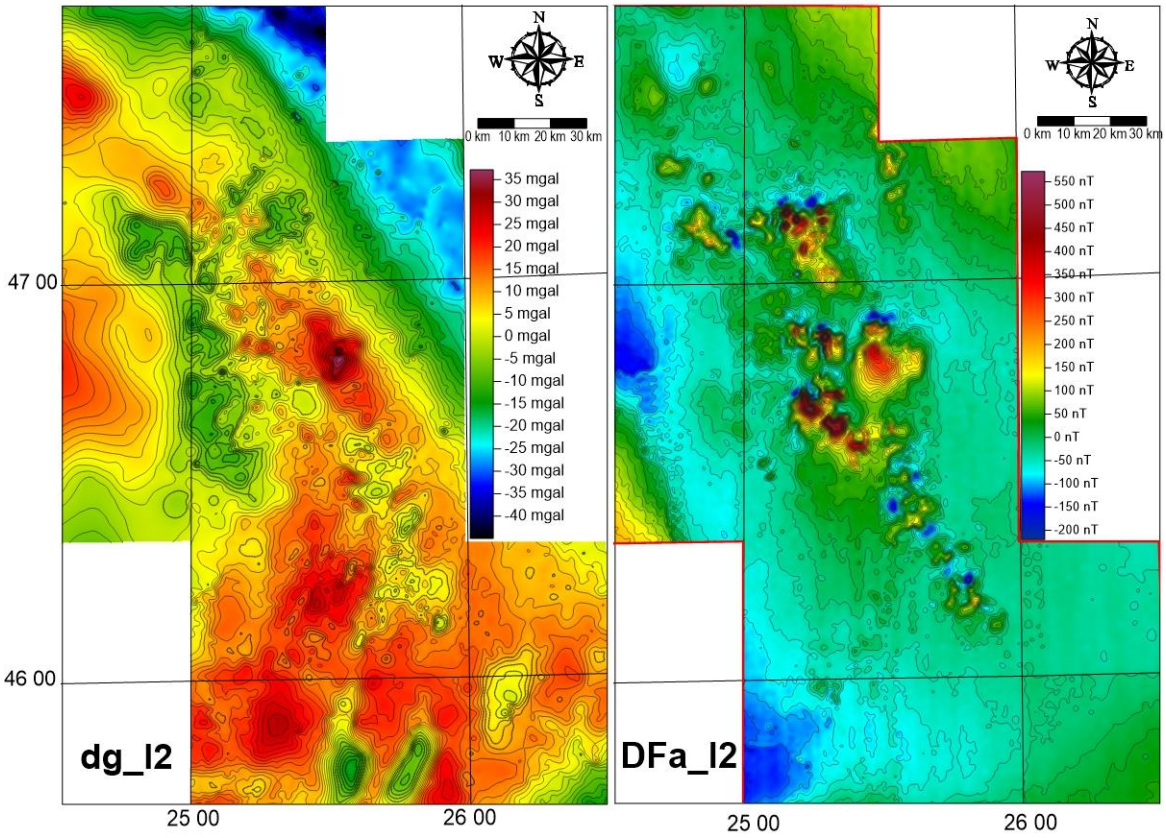

Fig. 4.4.1.2.3 Residual geomagnetic and Bouguer anomaly over the NQECV area.

Topography effects were also considered in assessing data quality especially for gravity information (Fig. 4.4.1.2.2.4)

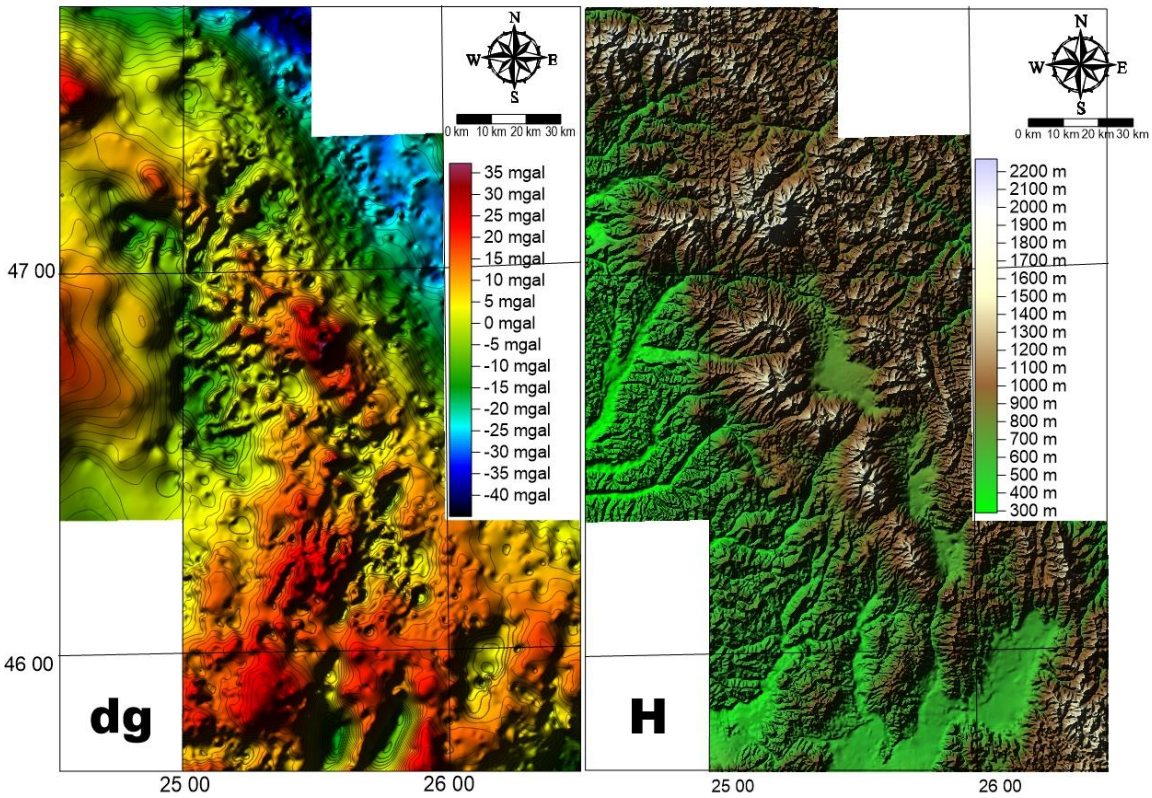

Fig. 4.4.1.2.3 Bouguer anomaly (2670 kg/m^3) pattern and topography of the NQECV area.

One of the first measures taken was changing the grid cell size to 5 km (the low-pass effect of the larger gridding is well known). Then, in order to improve the signal/noise ratio and provide more intuitive images, several filters (as described in the section 4.2.3) have been designed and applied. Next chapters report the results.

4.4.1.2.2. Geomagnetic field images

Fig. 4.4.1.2.2.1 shows the total intensity scalar geomagnetic anomaly within study area

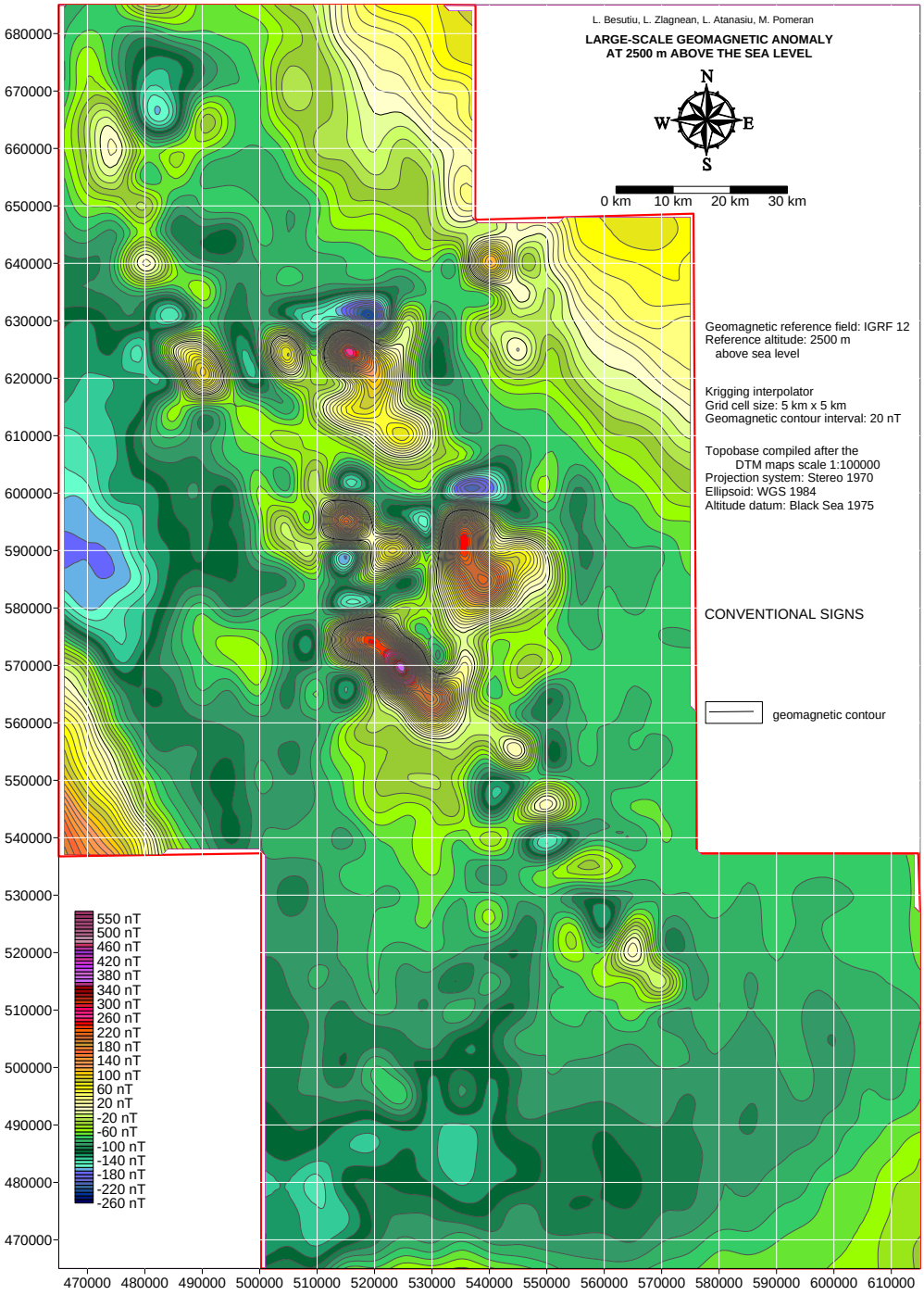

Fig. 4.4.1.2.2 The geomagnetic anomaly over NQECV on a plan situated at 2500 m above the sea level

For removing lateral effects, various reference fields have been designed an applied.

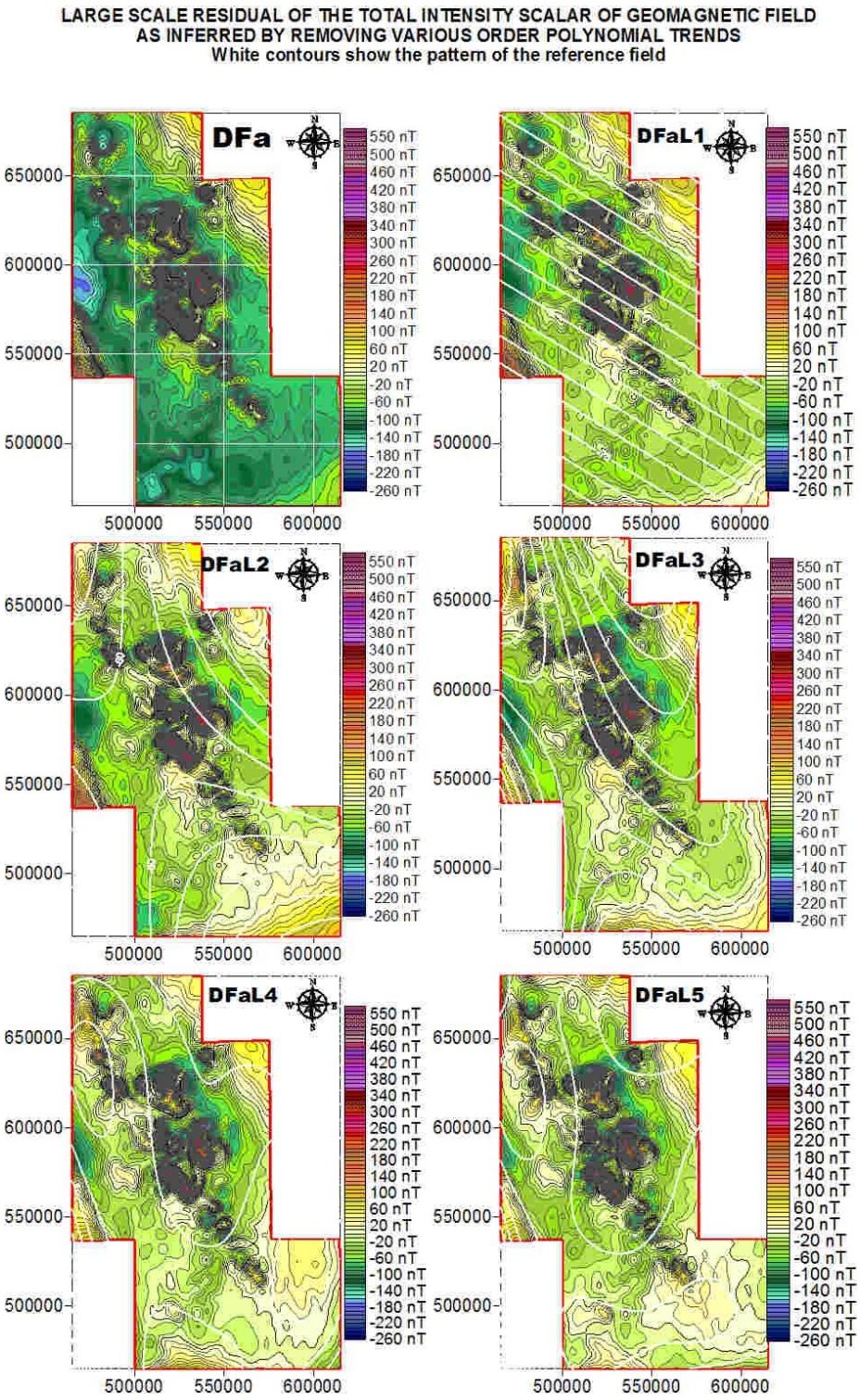

Fig. 4.4.1.2.3 Residual geomagnetic anomaly as obtained by removing some polynomial trends. White contours show the pattern of the reference fields.

The most balanced gravity anomaly has been provided by removing a second order polynomial trend from the observations (fig. 4.4.1.2.4).

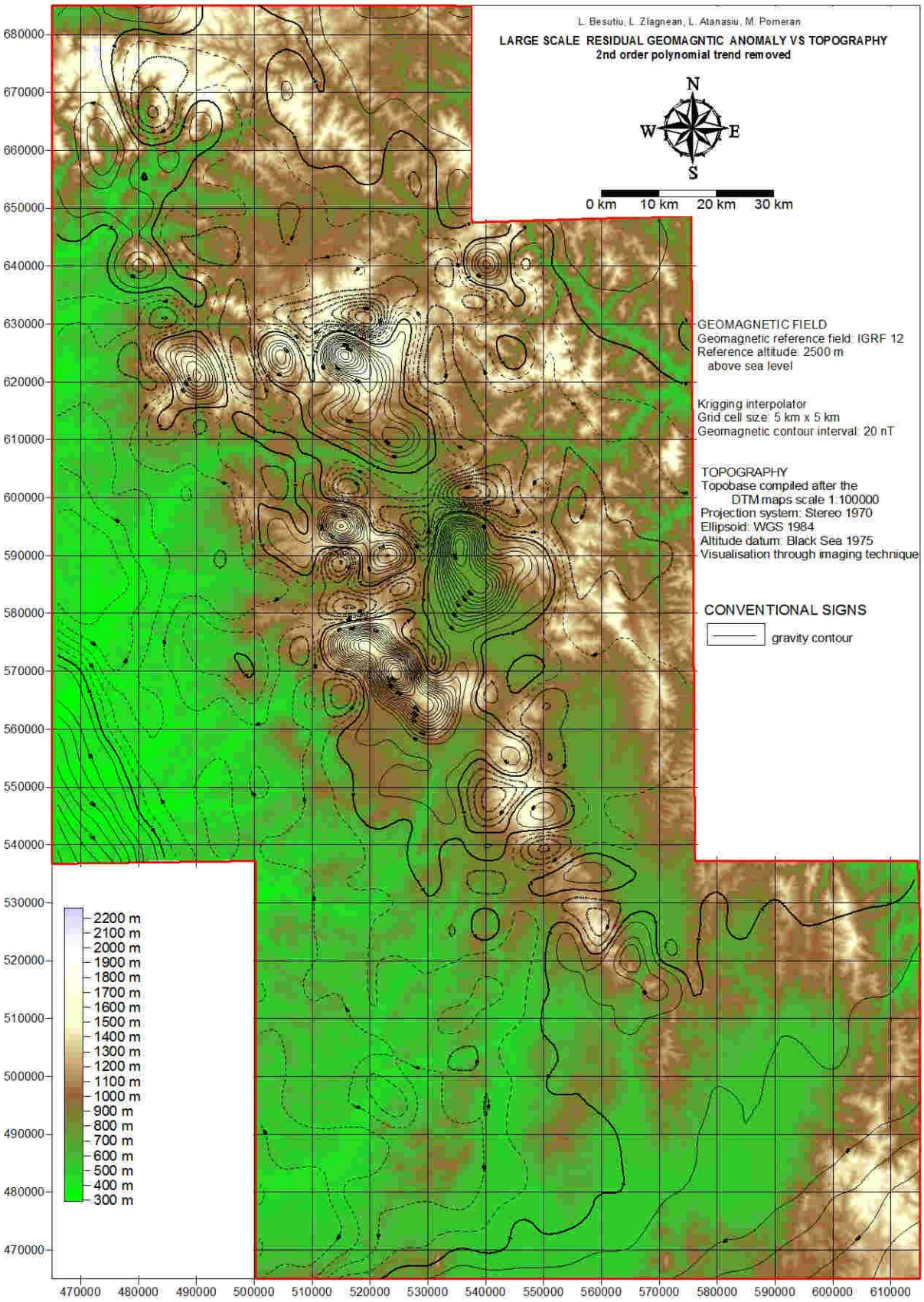

Fig. 4.4.1.2.4 Residual geomagnetic anomaly obtained by removing a second order polynomial trend from data on a plan located at 2500 m above the sea level vs topography

Various filters have then been applied to this anomaly in order to outline geomagnetic effects of NQECV.

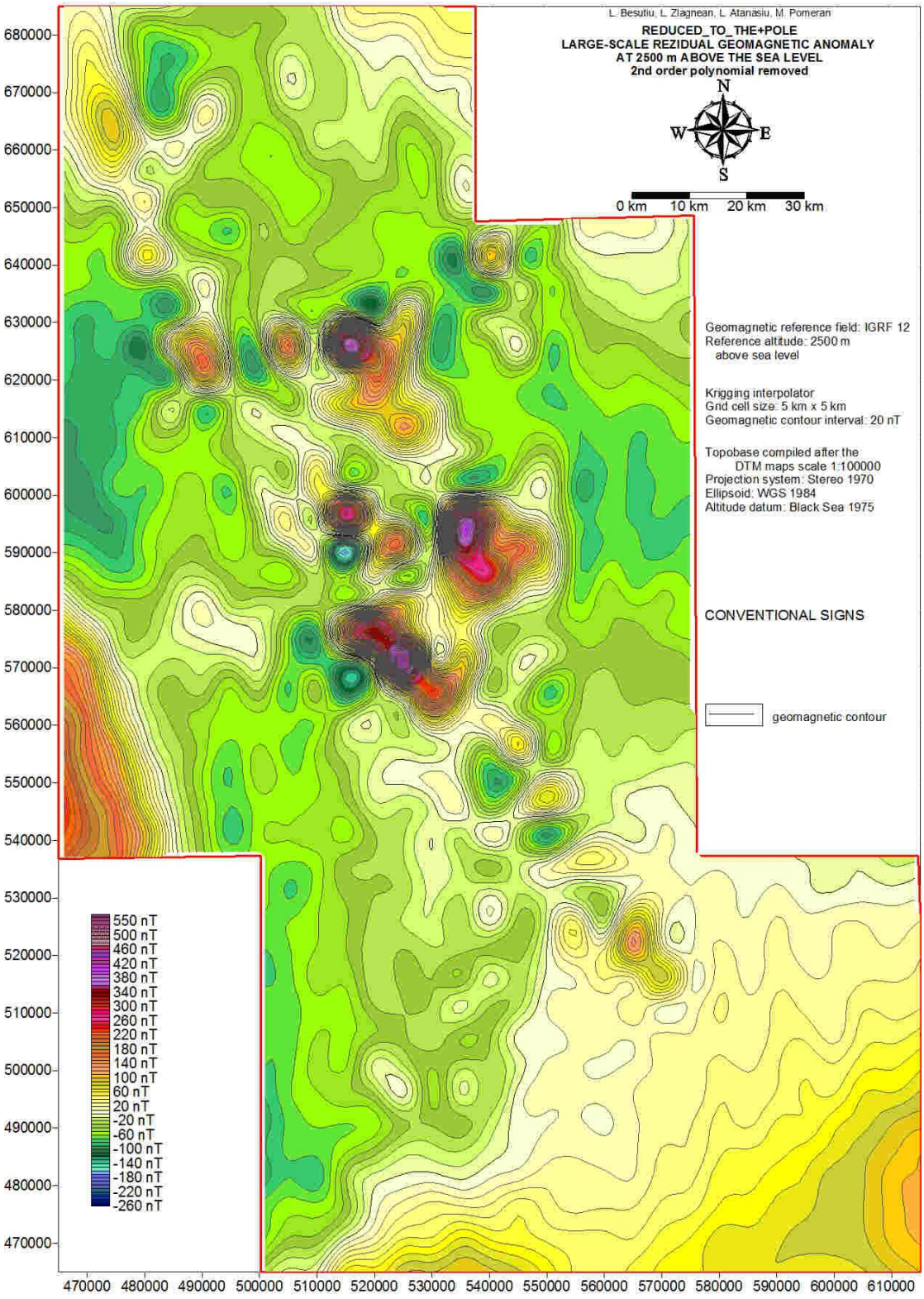

Fig. 4.4.1.2.5 Reduced to the pole residual geomagnetic anomaly

As observed, the large value of inclination (65°) implements only small differences between the reduced-to-pole geomagnetic anomaly and the initial data.

Figure 4.4.1.2.6 presents the horizontal gradient of the reduced-to-the-pole residual geomagnetic anomaly.

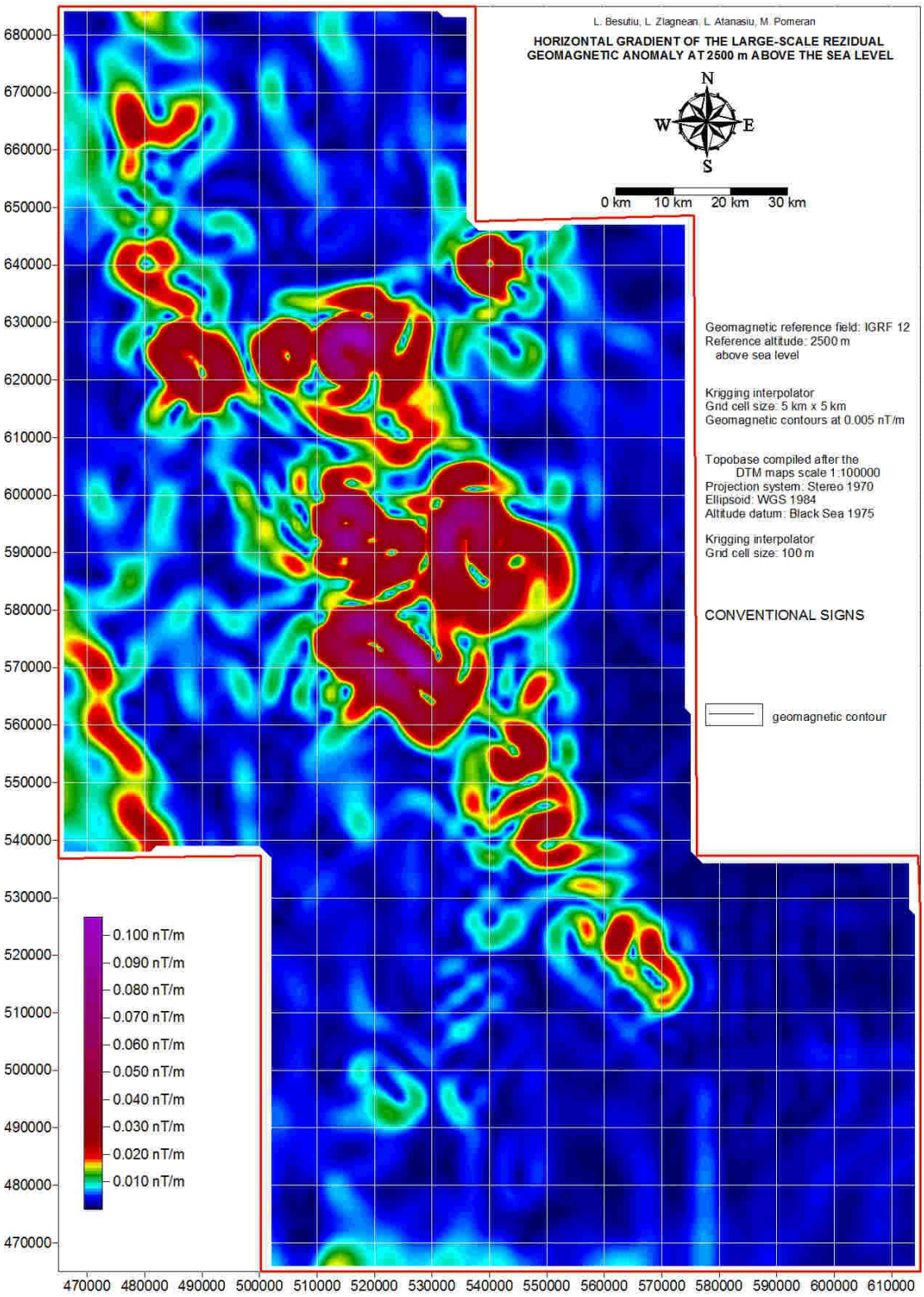

Fig. 4.4.1.2.6 Horizontal gradient of the reduced-to-pole residual geomagnetic anomaly within NQECV

Fig. 4.4.1.2.7 shows the vertical gradient of the reduced-to-the pole residual geomagnetic anomaly .

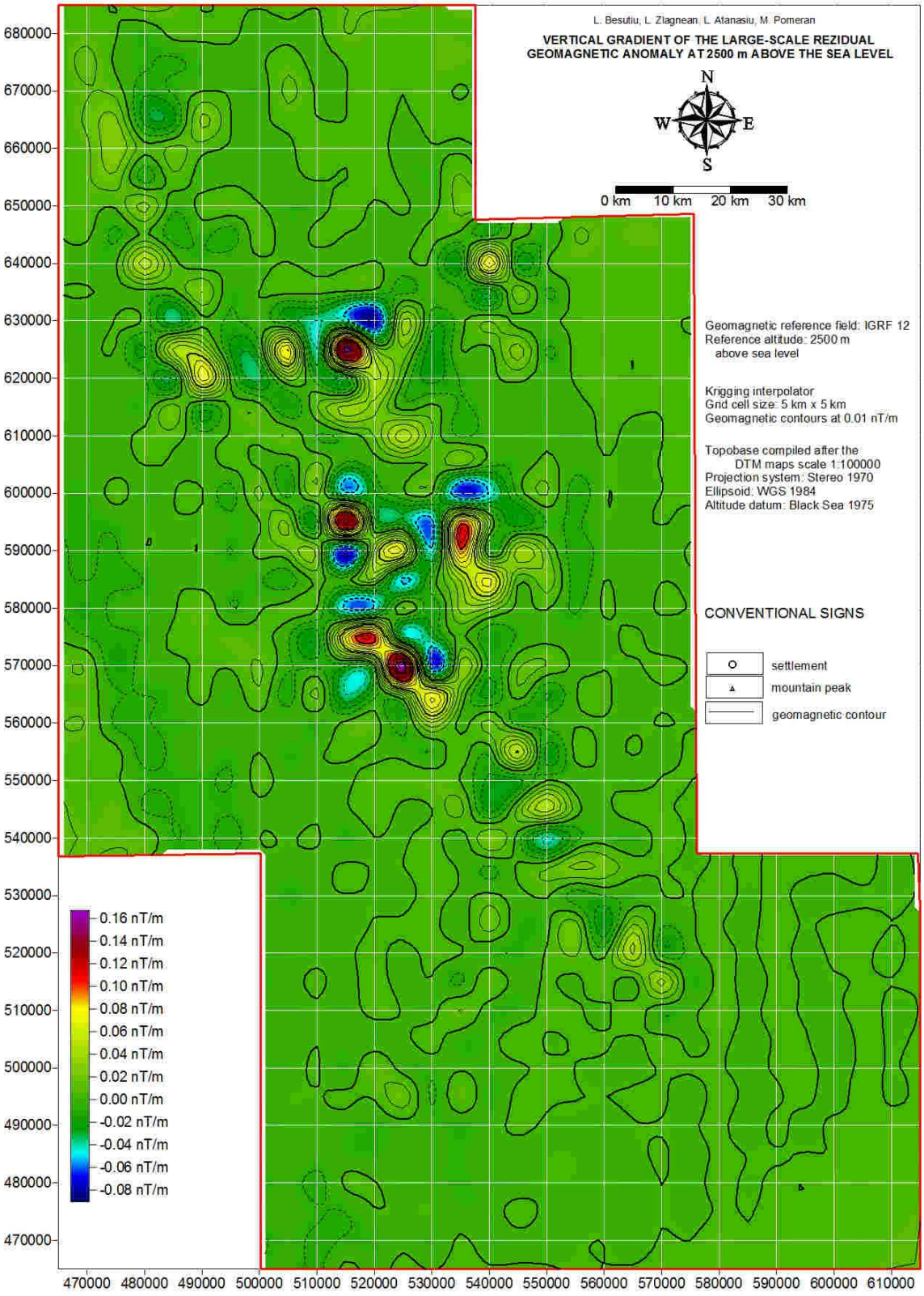

Fig. 4.4.1.2.7 Vertical gradient of the reduced-to-pole residual geomagnetic anomaly within NQECV

The vertical gradient emphasizes shallow sources being accurately located above them. Another operator that outlines the contour of geomagnetic sources very well is the analytical signal (Fig. 4.4.1.2.8).

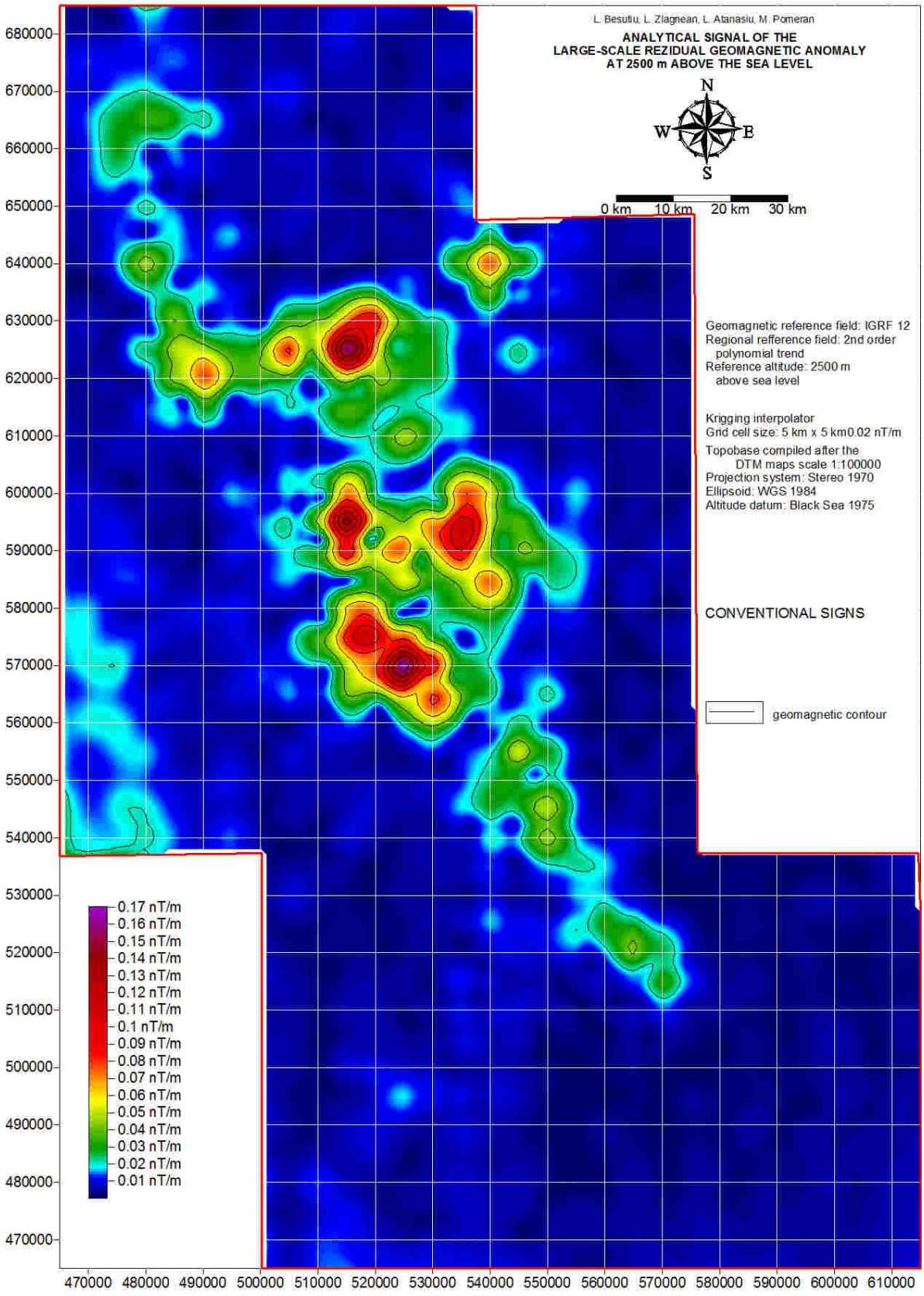

Fig. 4.4.1.2.8 The map of the analytical signal within NQECV

Starting from the geomagnetic data was also computed a map of pseudo-gravity (Fig. 4.4.1.2.9).

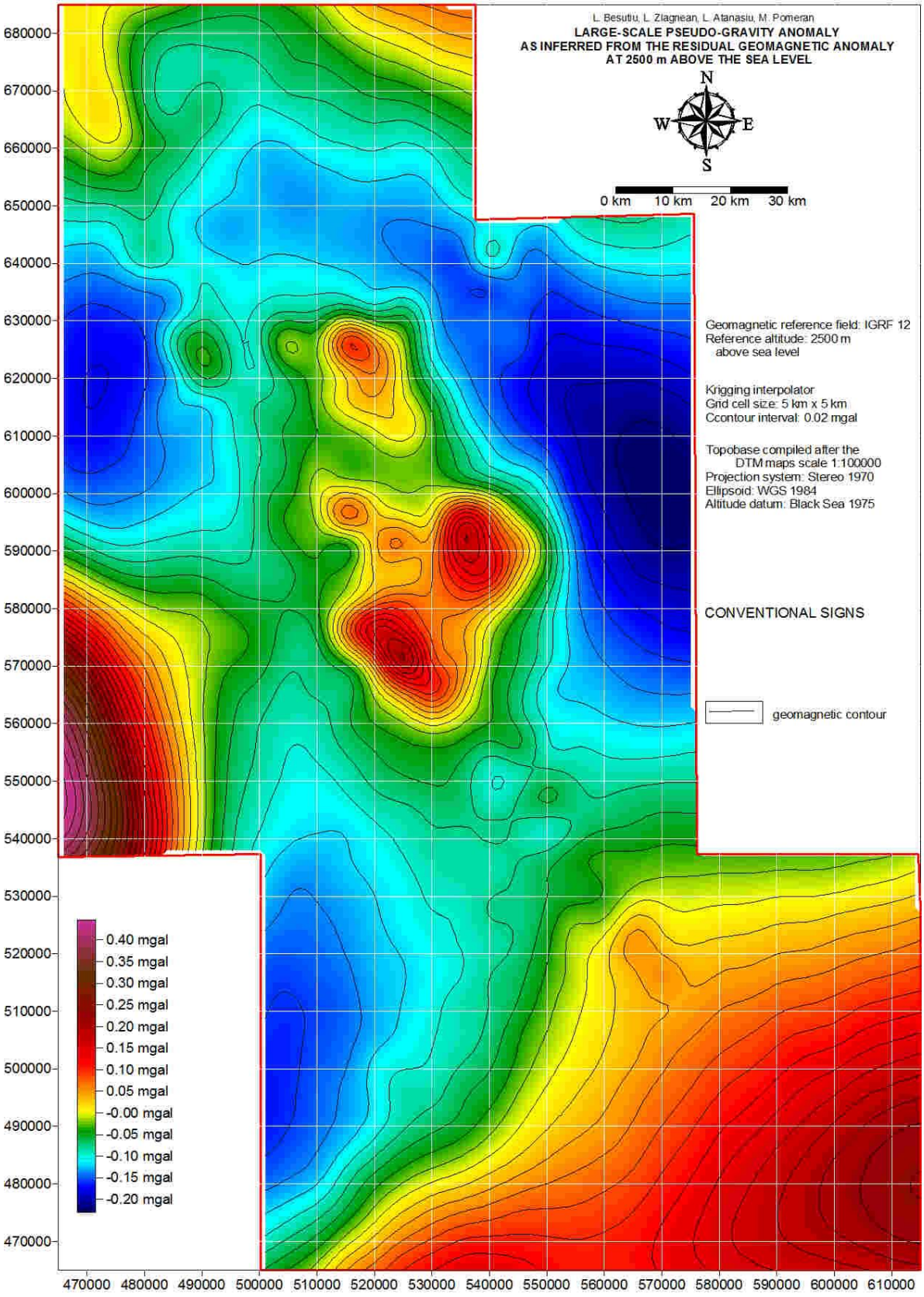

Fig. 4.4.1.2.9 Pseudo-gravity on a horizontal plan located at 2500 m above the sea level over NQECV

4.4.1.2.3. Gravity images

Like the geomagnetic anomaly, the Bouguer anomaly map has been reconstructed for a grid cell size of 5 km x 5 km. (Fig. 4.4.1.2.10)

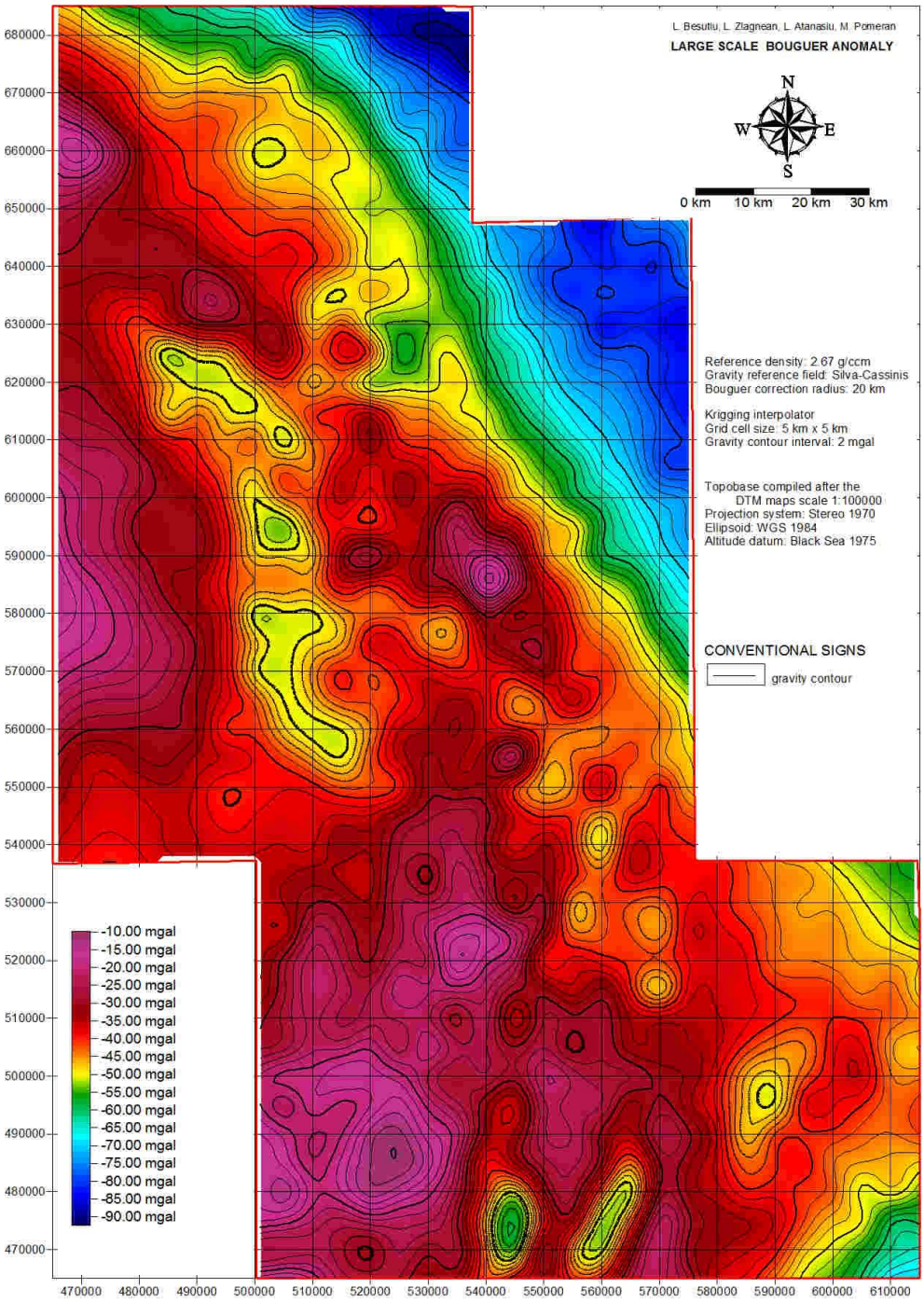

Fig. 4.4.1.2.10 Ground large scale Bouguer anomaly over the NQECV

The image is clearly affected by the mass deficits created by the East Carpathians foredeep and Transylvanian Basin deposits. After an analysis similar to that applied to

geomagnetic data, it has been decided removing a third order polynomial trend from the data produces the best balanced residual anomaly (Fig. 4.4.1.2.11).

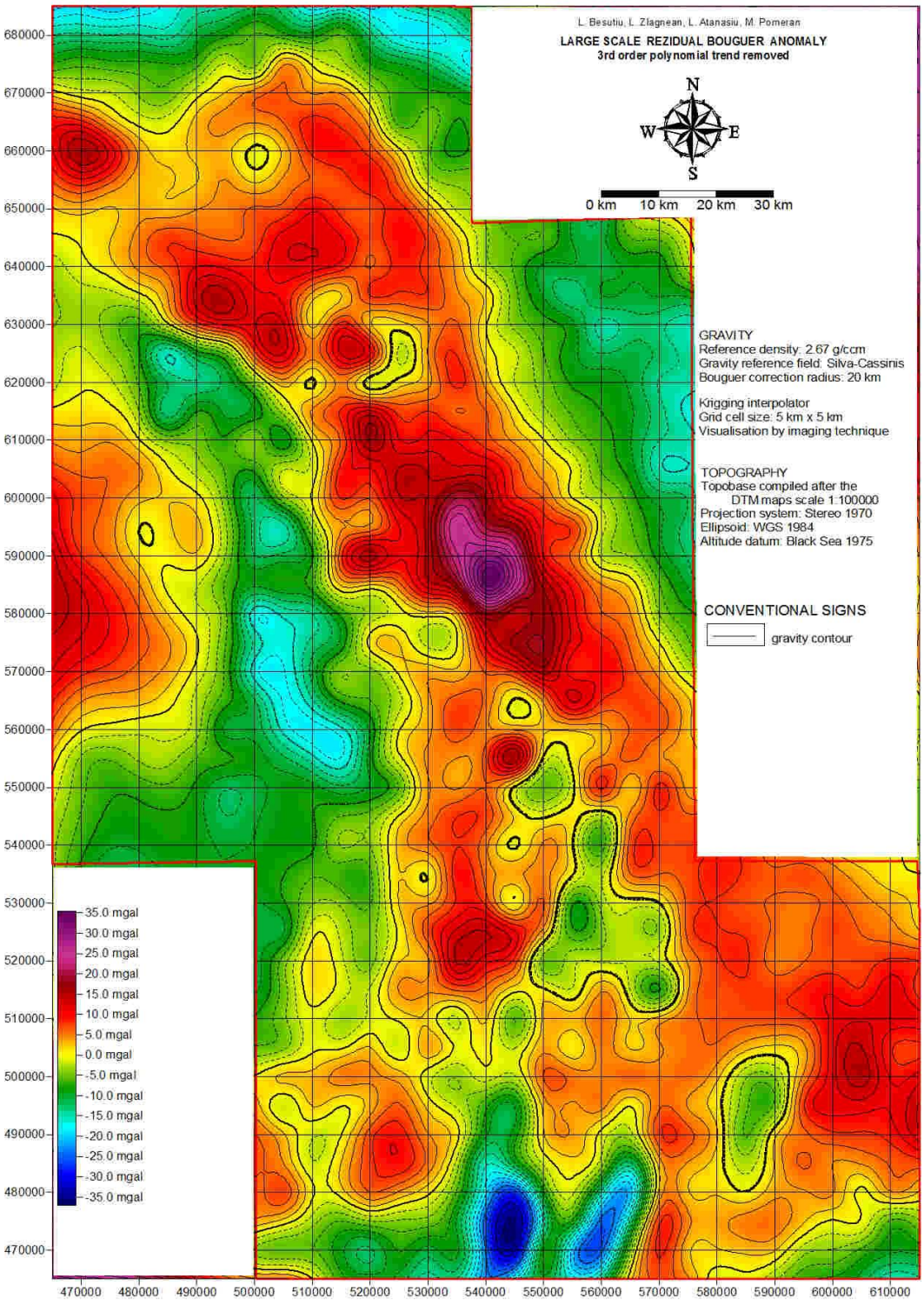

Fig. 4.4.1.2.11 Residual Bouguer anomaly obtained by removing a third order polynomial trend from observations

Fig. 4.4.1.2.12 shows correlation of this anomaly with the topography. The appropriateness of the reference density chosen (2670 kg/m^3) is obvious.

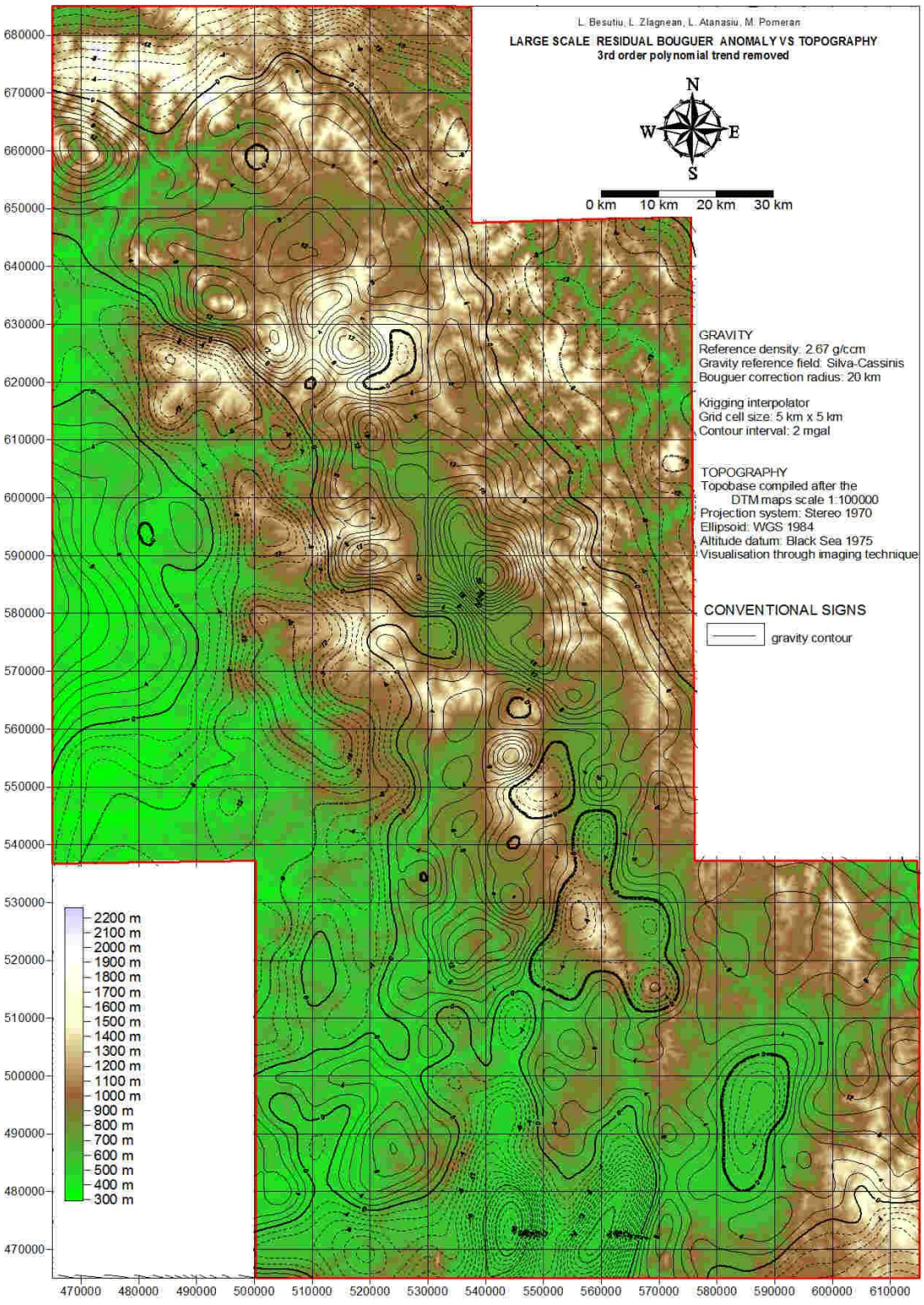

Fig. 4.4.1.2.13 Large-scale residual Bouguer anomaly obtained by subtracting a third order polynomial trend vs topography

This density has been also chosen for emphasizing the presence of the hidden intrusive rocks. The following figures show the results of filtering by employing the various operators mentioned previously.

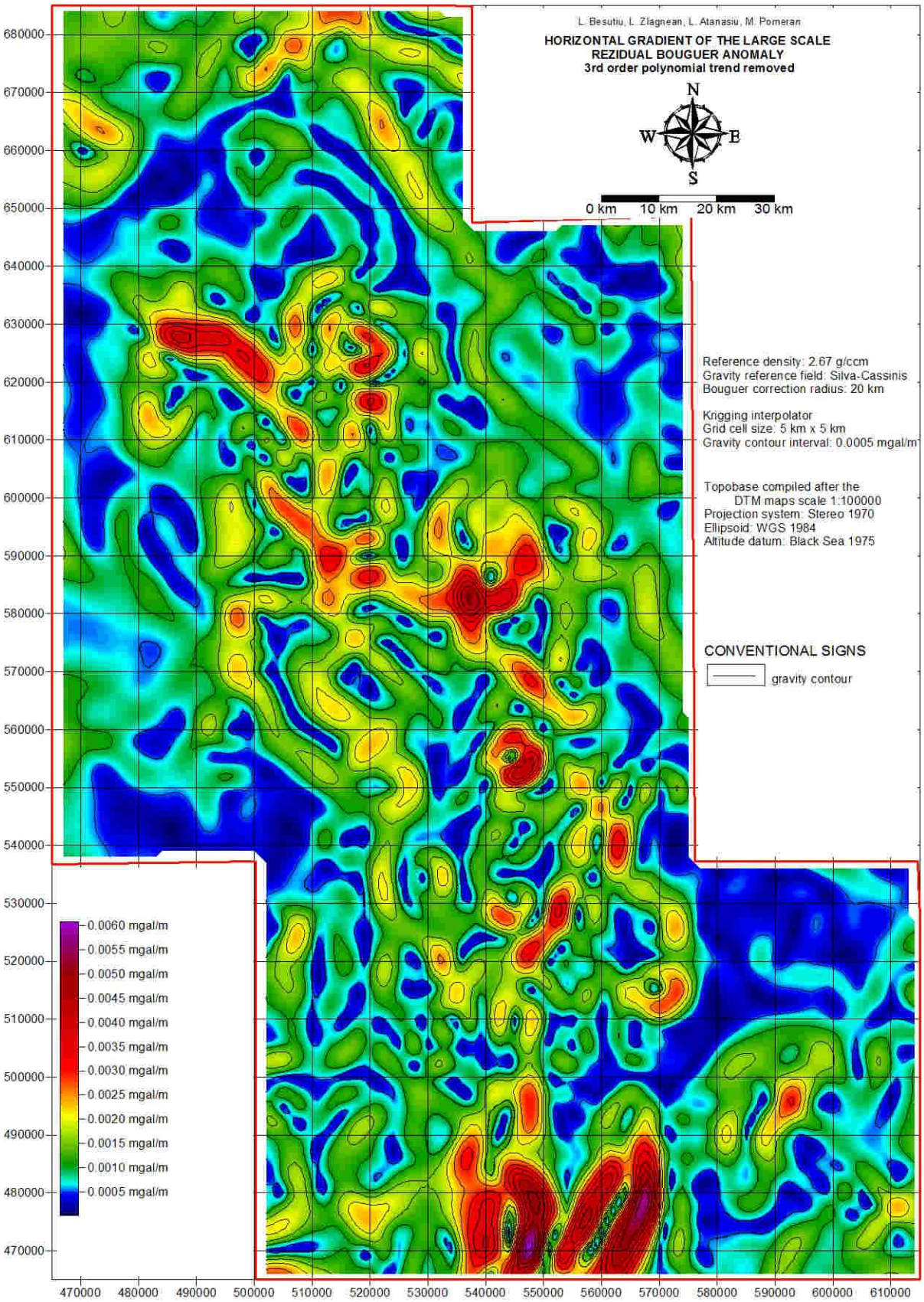

Fig. 4.4.1.2.14 Horizontal gradient of the large-scale residual Bouguer anomaly

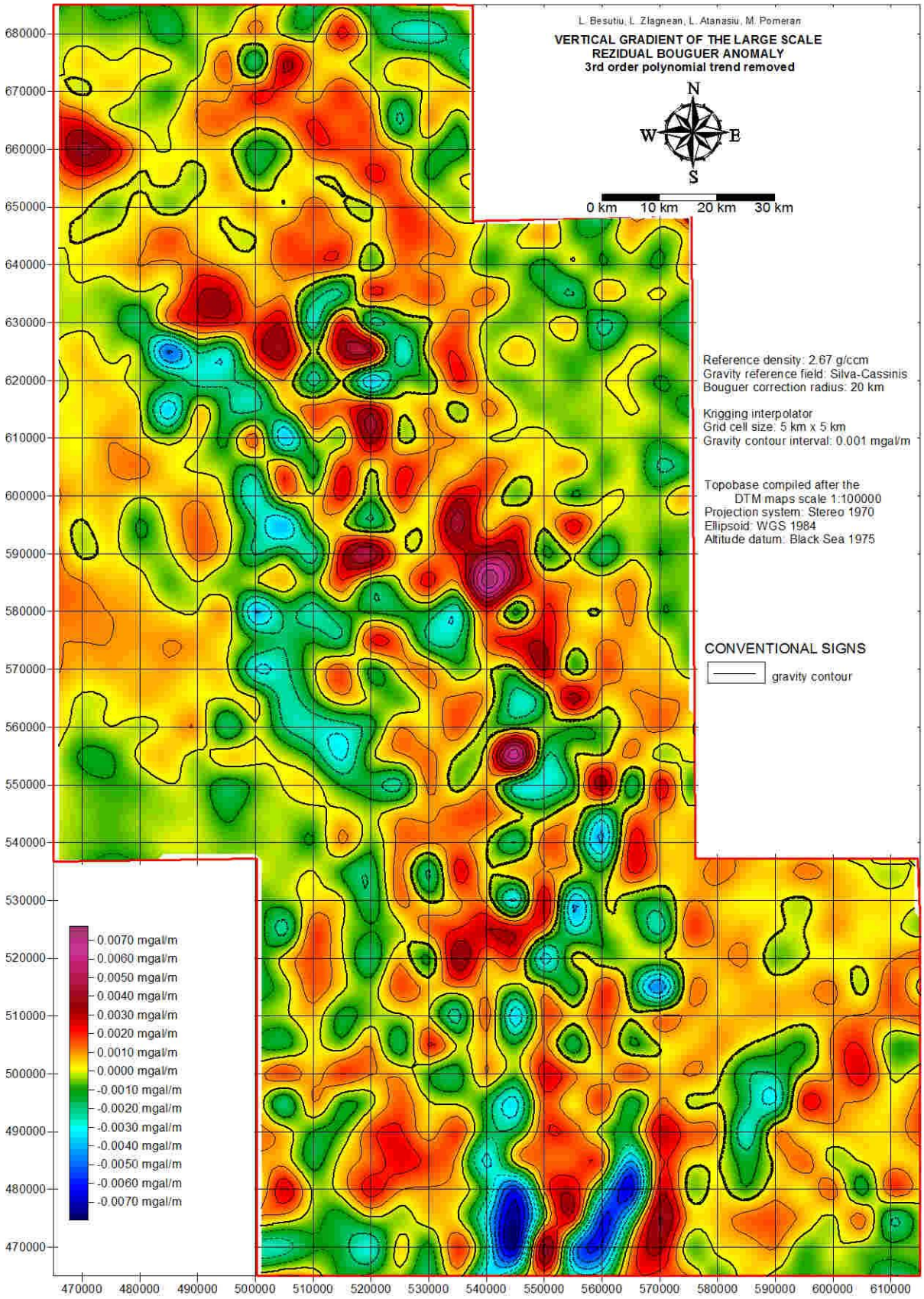

Fig. 4.4.1.2.15 Vertical gradient of the large-scale residual Bouguer anomaly

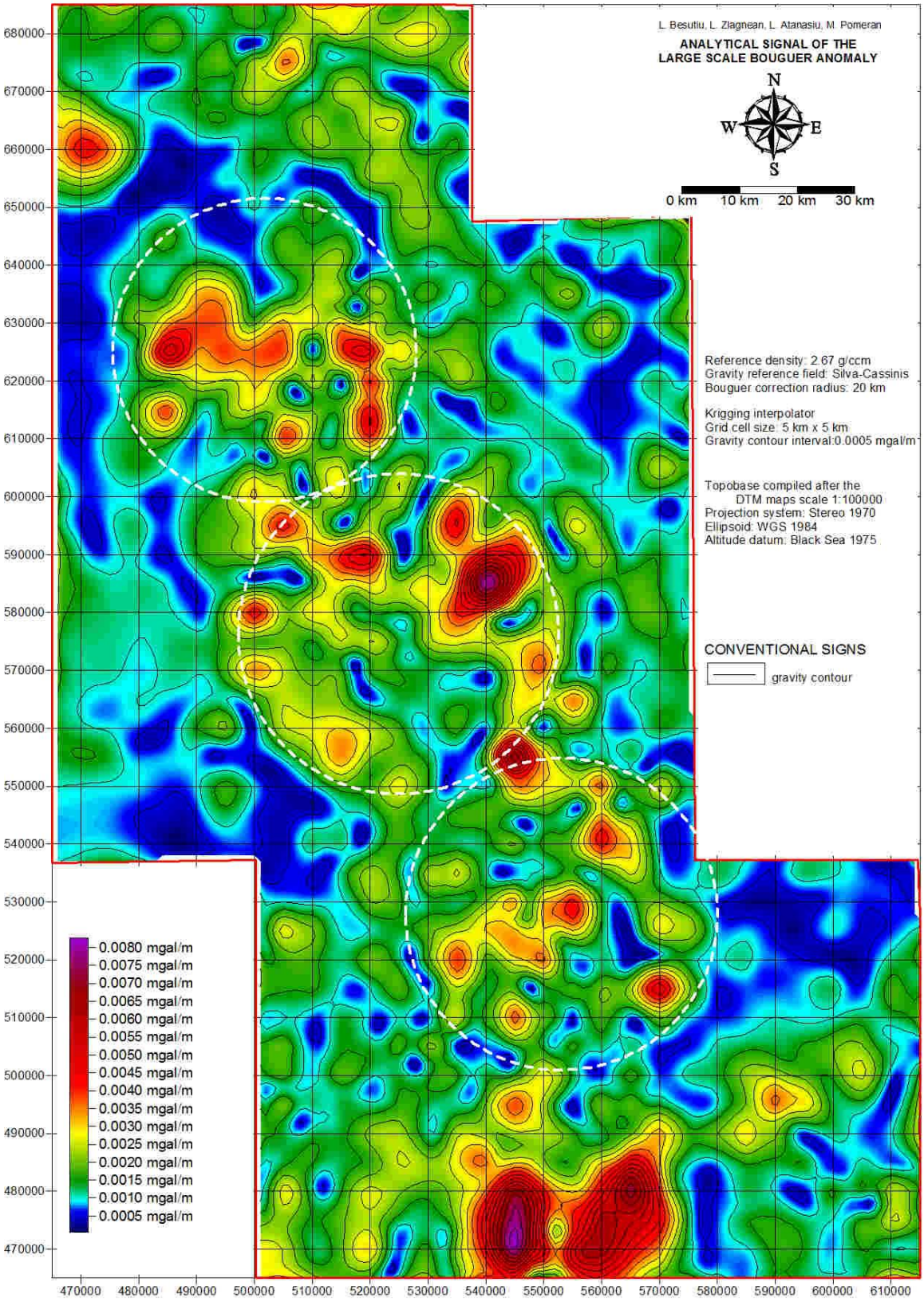

Fig. 4.4.1.2.16 Analytic signal the large-scale residual Bouguer anomaly

4.4.1.2.4. Power spectra

Power spectra represent a valuable indicator reflecting some significant parameters of the sources of the geomagnetic and gravity anomalies like burial depth, field energy and volumes involved. Figure 4.4.1.2.4.1 presents power spectra and burial depth of the sources of the gravity and geomagnetic field within NQECV area.

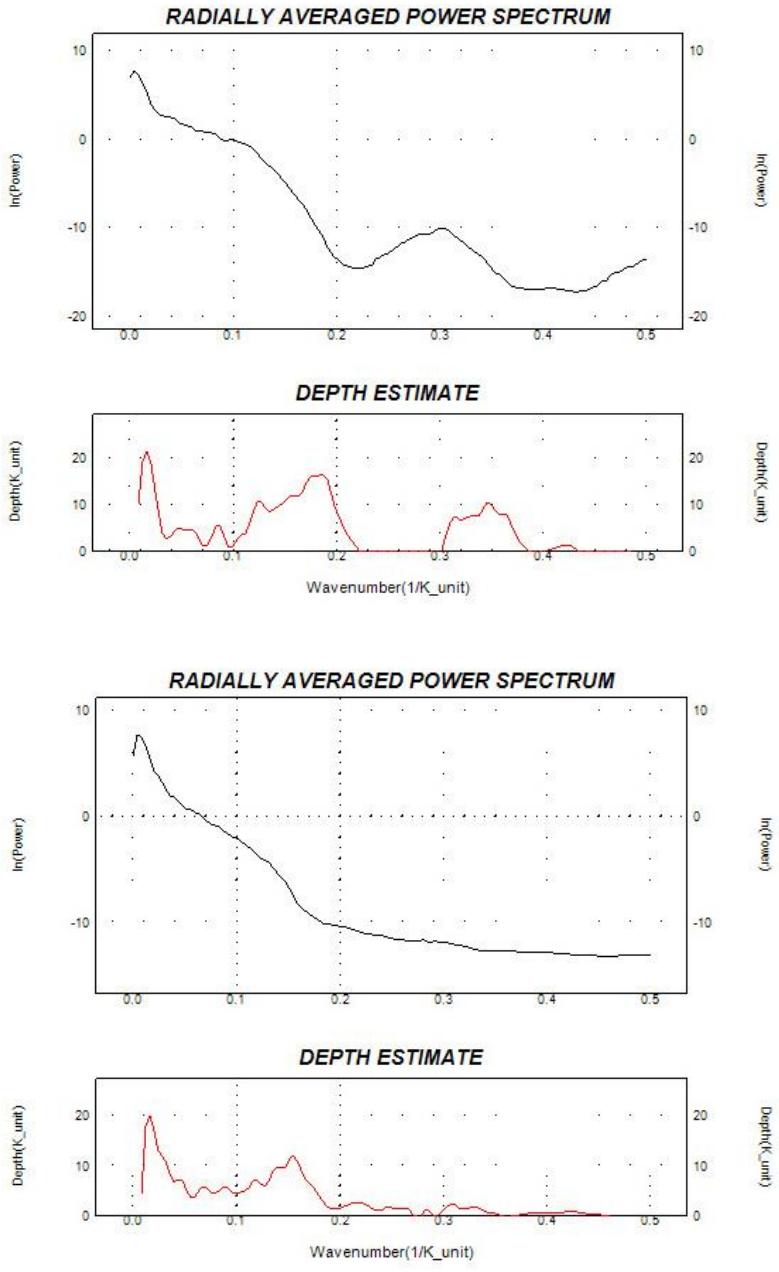

Fig. 4.4.1.2.4.1 Power spectra an in-depth location of sources of the large scale geomagnetic anomaly (above) and Bouguer anomaly (below)

Next step consisted in the analysis of the power spectra of the residual anomalies. We started with the analysis of the reference fields (fig. 4.4.1.2.2)

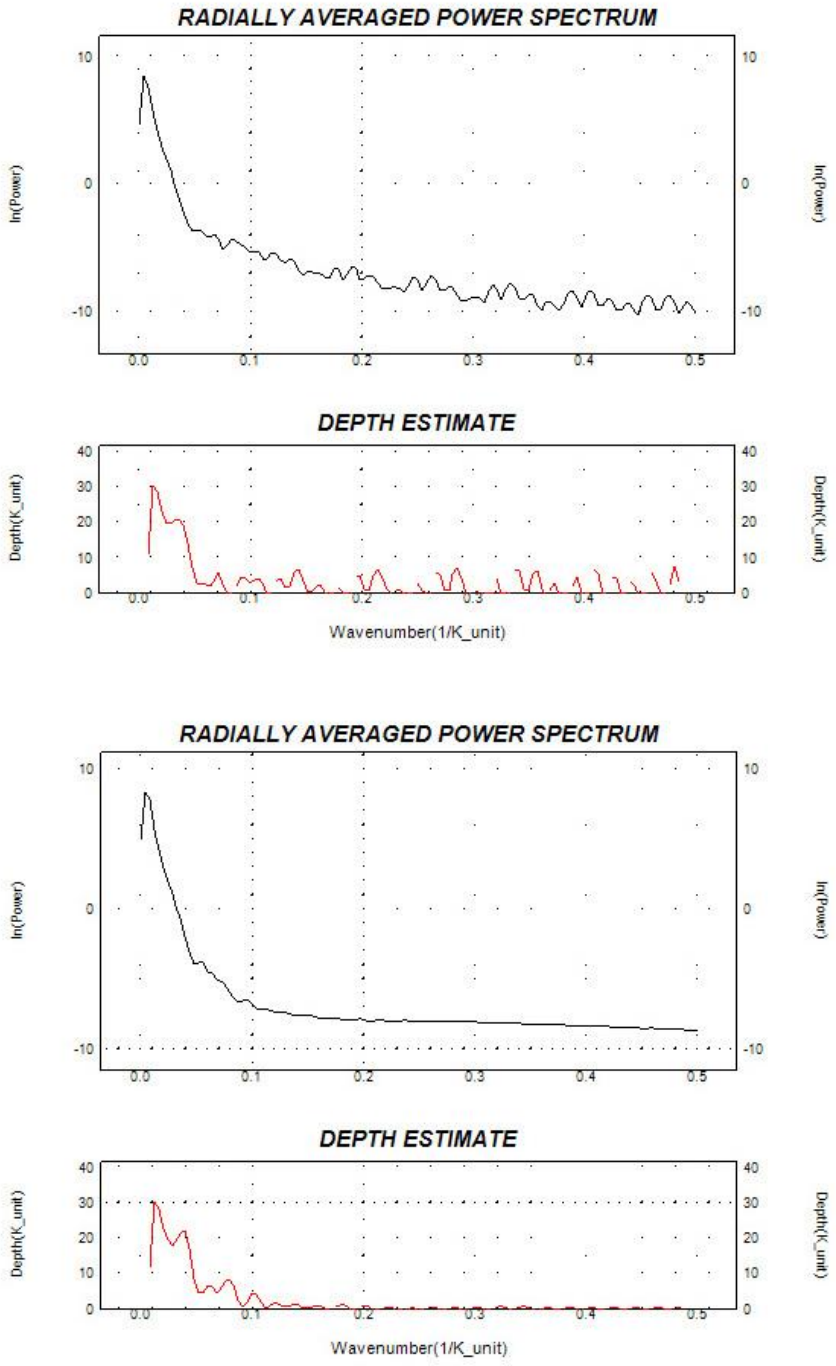

Fig. 4.4.1.2.4.2 Power spectra of the regional reference fields used in computing residual anomalies of the gravity and geomagnetic field

Figure 4.4.1.2.4.3 shows the average radial power spectra of the residuals obtained after removing the regional reference fields.

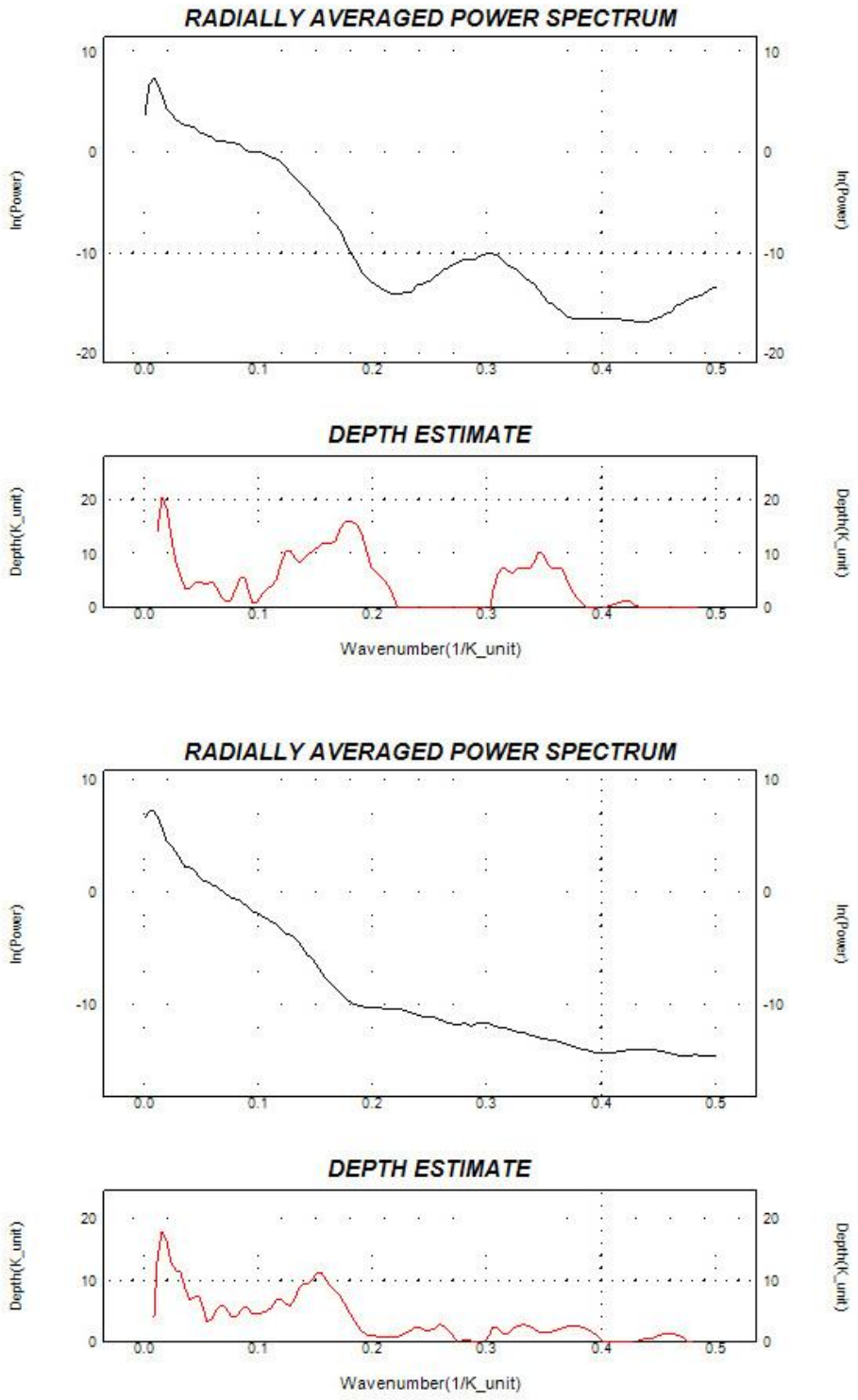

Fig. 4.4.1.2.4.3 Average radial power spectra of the geomagnetic versus gravity field
Above: average radial power spectra of the residual geomagnetic anomaly. Below: average radial power spectra of the residual Bouguer anomaly.

Interesting results were obtained when distinctly computing power spectra of the gravity field over NQECV major districts: Calimani, Gurghiu, Harghita Nord and Harghita Sus (Fig. 4.4.1.2.4.4).

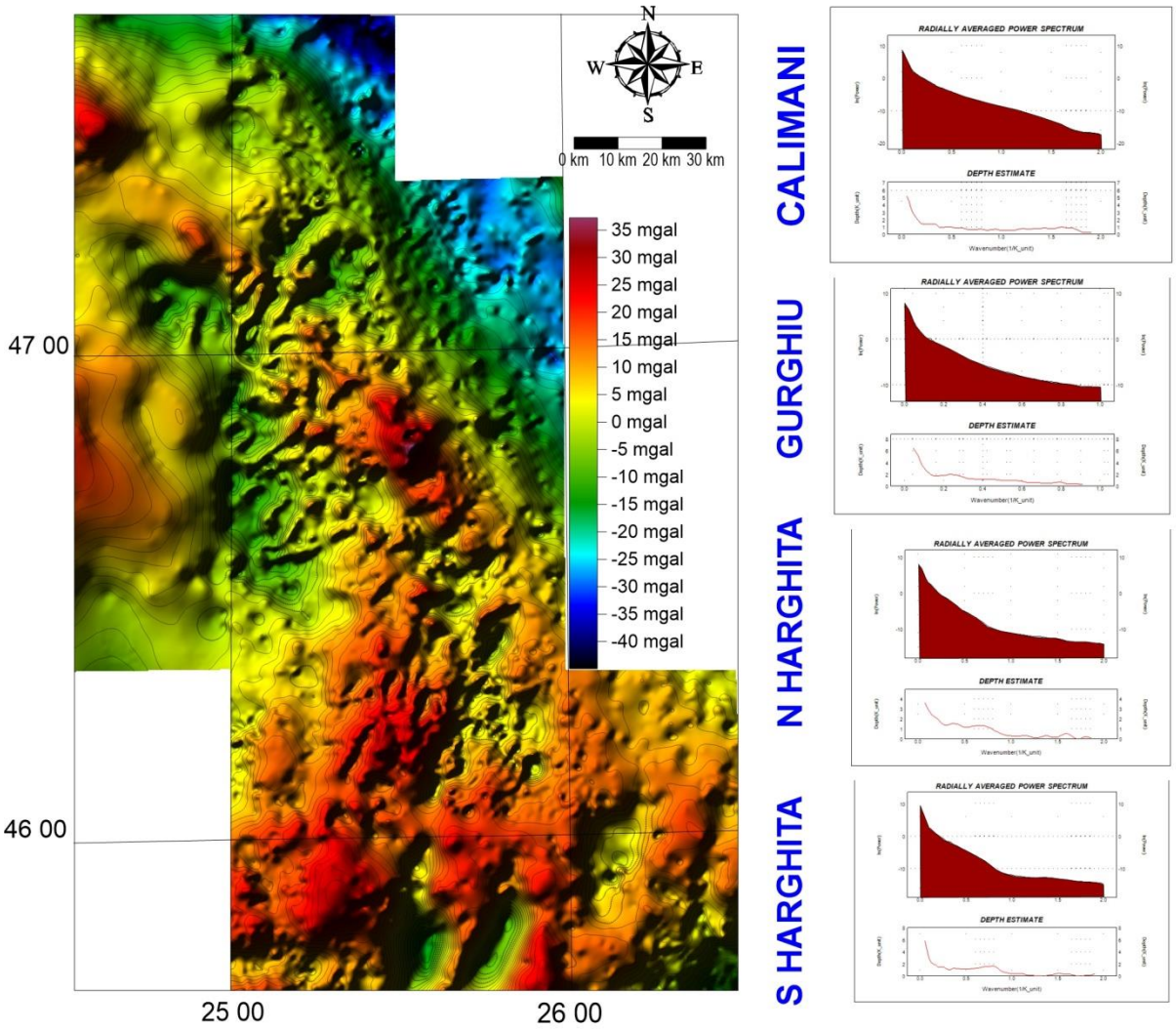

Fig. 4.4.1.2.4.4 Bouguer anomaly within INSTEC area and power spectra computed for major districts (Calimani, Gurghiu, Harghita N and Harghita S)

It is obvious from the graphs presented on the left side that the gravitational energy is progressively decreasing from Călimani to South Harghita, as an evidence of decrease of the volumes released by volcanism in different areas. This observation is fully consistent with previous assumptions claiming a progressive lowering of volcanic activity along the volcanic chain from north to south.